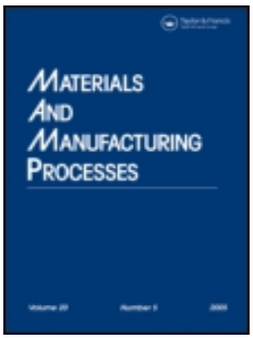

Materials and Manufacturing Processes

ISSN: 1042-6914 (Print) 1532-2475 (Online) Journal homepage: www.tandfonline.com/journals/lmmp20

A Methodology for Cutting Force Prediction in Side Milling

Mehmet Aydın, Mehmet Uçar, Abdulkadir Cengiz, Mustafa Kurt & Barkın Bakır

To cite this article: Mehmet Aydın, Mehmet Uçar, Abdulkadir Cengiz, Mustafa Kurt & Barkın Bakır (2014) A Methodology for Cutting Force Prediction in Side Milling, Materials and Manufacturing Processes, 29:11-12, 1429-1435, DOI: 10.1080/10426914.2014.912315

To link to this article: https://doi.org/10.1080/10426914.2014.912315

Materials and Manufacturing Processes, 29: 1429–1435, 2014

ISSN: 1042-6914 print/1532-2475 online
DOI: 10.1080/10426914.2014.912315

Taylor & Francis
Taylor & Francis Group

A Methodology for Cutting Force Prediction in Side Milling

Mehmet Aydin[1], Mehmet Uçar[2], Abdulkadir Cengiz[3], Mustafa Kurt[4], and Barkin Bakir[5]

[1]*Mechanics Program, Bilecik Şeyh Edebali University, Bilecik, Turkey*
[2]*Department of Automotive Engineering, Kocaeli University, Kocaeli, Turkey*
[3]*Department of Mechanical Education, Kocaeli University, Kocaeli, Turkey*
[4]*Department of Mechanical Engineering, Marmara University, İstanbul, Turkey*
[5]*Department of Mechanical Education, Marmara University, İstanbul, Turkey*

This article describes a methodology based on force distributions for predicting cutting forces in side milling 7075-T651 aluminum. The methodology includes a practical mechanism for gathering experimental data. Milling forces on each disc are measured by experimentally dividing the cutter into discs for determining the milling coefficients. Force distributions are characterized as functions of cutting and edge forces, including cutter geometry and cutting parameter effects. In contrast to previous researches, the coefficients are determined considering relations between load and shear. Owing to its high performance, this methodology can be effectively used to improve machining accuracy in side milling.

Keywords Aluminum; Design; Forces; Milling; Parameters; Processes; Simulation; Tooling.

Introduction

Side milling is a greatly utilized material removal application for manufacturing 2D contour parts in dies and molds industry. Interactions between workpiece and helical flutes generate cutting forces. Accurate and reliable force predictions are essential to enhance processing efficiency. The selection of optimum cutting conditions is very important to increase processing efficiency [1]. Force predictions also have a critical effect in achieving the desired surface quality since surface properties affect dimensional accuracy, friction, wear as well as functions of mechanical products [2].

Analytical and semi-analytical predictions of milling forces have been studied to provide a basic understanding to process planners in selecting cutting conditions. Li et al. [3] modeled milling forces by developing a simulation approach based on a well-known metal cutting assumption. Decomposing end mill into segments in this approach, the actions of segments were considered as oblique cutting. Fontaine et al. [4] proposed an approach to estimate milling forces from an oblique cutting model built by material and friction attributes for surface milling. This approach also relies on oblique cutting processes described by tooth segments. Sun et al. [5] predicted cutting forces depending on the cutter–workpiece motion in sculptured surface machining. The forces were calculated by establishing relations between milling coefficients and chip thickness. Hosseini et al. [6] developed a method predicting cutting forces by calculating chip load for end mills with various geometrical variables. This method identifies process geometry from flute points. Wan et al. [7] established a unified approach to predict milling forces for helix tool geometries. They determined shear stress, shear, and friction angles needed for force predictions through milling tests instead of orthogonal turning ones.

Efficiently establishing the milling coefficients affecting the accuracy of cutting forces constitutes an important research subject. Dotcheva et al. [8] evaluated milling coefficients through measured surface error. For this purpose, they established a mechanism consisting of two strips with different axial depths and the same cutting parameters. Wan et al. [9, 10] suggested a procedure to calibrate milling coefficients using instantaneous cutting forces. They stated that several tests were required for determining the milling coefficients as functions of instantaneous chip thickness. Budak et al. [11] established an approach to determine milling coefficients from the oblique cutting theory with orthogonal cutting quantities. The results indicated that this approach provides a way for predicting milling coefficients in end milling. Gonzalo et al. [12, 13] offered inverse approaches decreasing the experimental study to evaluate milling coefficients. They implemented two methods based on orthogonal and oblique cutting simulations, and milling tests not dependent on radial cut depth for determining the coefficients. Wang et al. [14] presented inverse proportion models to predict milling coefficients from simulation tests. They utilized the milling forces obtained from the suggested model to optimize process conditions.

In recent years, micro milling has been applied in mechanical component production. However, the ratio of feedrate to cutter radius causes error in predicted

Received January 27, 2014; Accepted March 5, 2014

Address correspondence to Mehmet Aydın, Mechanics Program, Bilecik Şeyh Edebali University, Bilecik, Turkey; E-mail: mehmet.aydin@bilecik.edu.tr

Color versions of one or more of the figures in the article can be found online at www.tandfonline.com/lmmp.

cutting forces [15]. Srinivasa and Shunmugam [16] included the edge radius and material strength to the mechanistic model for predicting micro end-milling forces. Those make it unusual from classic helical milling in determining milling coefficients. Rao and Shunmugam [17] predicted micro end-milling forces with an approach that relies on forces acting on tooth segments and milling coefficients evaluated implementing the oblique cutting analysis. In this approach, the forces were associated with the uncut chip area. Afazov et al. [18] predicted micro milling forces for AISI H13 steel using a method depending on the chip thickness obtained from the mechanics of milling cutter and the forces computed with finite element analysis. Özel and Liu [19] introduced an operation designing model to achieve predefined milling forces, surface accuracy, and roughness during the machining of micromold cavities. The model was used to identify machining conditions on molds.

Despite the utility of the methods presented above for defining milling coefficients, they do not include the effects of force distribution along the flute. New mechanisms are necessary to facilitate applications and enhance the prediction accuracy. Therefore, the aim of this study is to develop a methodology that can be readily implemented for determining milling coefficients. For this purpose, a new and practical calibration mechanism is established, which can experimentally divide the cutting part of the end mill into discs. The mechanistic model is then extended to predict the milling forces in side milling. The advantage of the suggested methodology is that the milling coefficients, including the effects of cutting parameters and cutter geometry, are calibrated by identifying the force distribution as the functions of cutting and edge forces on each disc. This can provide useful process information to manufacturing engineers for achieving dimensional accuracy required in side milling. The performance of the methodology is confirmed by experimental tests performed on 7075-T651 aluminum.

Proposed methodology

This study introduces two different novelties for force predictions in end milling. First, a new mechanism is designed to perform calibration tests, which can experimentally discretize the cutter along its z-axis. The mechanistic model is then improved by determining the milling coefficients, which involve the effects of cutting and edge force distributions.

Experimental work

Milling tests were conducted on a Johnford VMC-550 machining center. The tests were performed on Al7075-T651 sheet metal slices with dimensions 50 mm × 250 mm × 3 mm. One-fluted carbide end mills with helix angle 30°, normal rake angles (γ_n) 5, 10, and 15°, and diameters (D) 8, 10, and 12 mm without any coating were used to identify the capability of the suggested methodology. Feed (F_X) and transverse (F_Y) forces were measured using the dynamometer 9443B.

Milling tests were performed at constant cutting speed (V) 30 m/min with three different feedrates (f_t) of 0.04, 0.08, and 0.12 mm/tooth without coolant. The axial cut depth was 1.5 times greater than the cutter diameter.

Experimental Mechanism

Force predictions still depend on milling coefficients defined from experimental data although various mechanistic models are developed for predicting milling forces. The approach widely used for defining the milling coefficients relies on measuring cutting forces for one tooth period. The variation of forces along the flute is further neglected for defining the milling coefficients. However, tangential and radial forces vary along the flute since the helix angle of flutes produces variation on the cutting force distribution along the z-axis [20]. Hence, the determination of milling coefficients requires the understanding of the force distribution for accurate model calibration.

A practical mechanism is here established to mechanistically calibrate the milling coefficients, which allows identifying the force distribution. For this purpose, the cutter is experimentally sliced into v number of disc elements over the axial cut depth. Figure 1 depicts the calibration mechanism. The workpieces are sheet metal slices, and blocks consisting of the slices placed on each other are constituted to identify the force distribution. One of the slices is clamped on the dynamometer. The others are mounted on the worktable. The lower tip of the end mill is initially located a few millimeters (d_{pos}) down from the bottom slice for stable cutting.

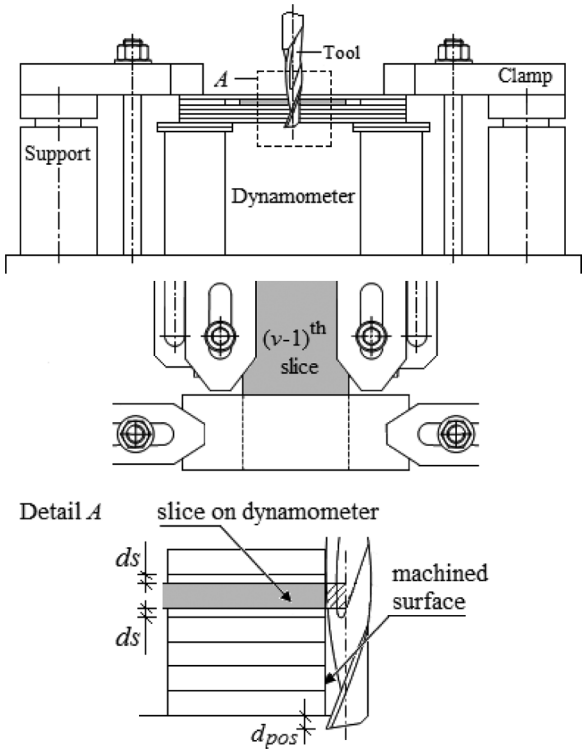

Figure 1.—Setup of calibration tests.

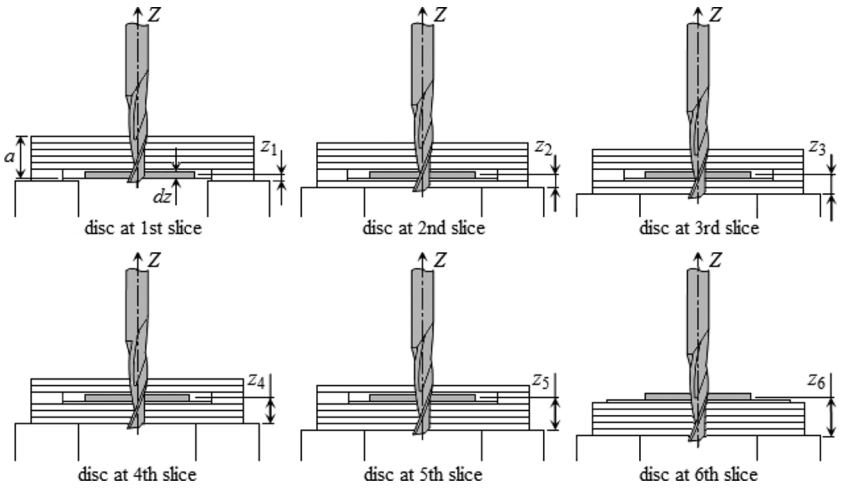

FIGURE 2.—Process of force distribution identification.

Experimental Procedure

A series of half-immersion up and down milling tests was conducted using the experimental mechanism developed. The average forces for each feedrate were found. The measured forces were obtained from the slice on the dynamometer despite machining all slice surfaces during tests. That is provided by leaving a gap (ds) between the slice on the dynamometer and others. The machining procedure was realized by changing the axial positions of the cutter and the slices on the worktable to identify cutting forces on each disc. The cutter axial increment is equal to the disc height dz. The determination of the force distribution for the $D = 12$ mm cutter is represented in Fig. 2. After collecting the force data, the coefficients are evaluated by implementing the model defined in the next section.

MODELING OF MILLING FORCES

Based on the work of Budak et al. [11], tangential ($F_{jz,T}$), radial ($F_{jz,R}$), and axial ($F_{jz,A}$) milling forces exerted by the element (dz) of the jth flute at axial position z are expressed as

$$\left.\begin{aligned} F_{jz,T}(\theta) &= [K_{\mathrm{Tc}}\, h(\theta_{jz}) + K_{\mathrm{Te}}]\, dz \\ F_{jz,R}(\theta) &= [K_{\mathrm{Rc}}\, h(\theta_{jz}) + K_{\mathrm{Re}}]\, dz \\ F_{jz,A}(\theta) &= [K_{\mathrm{Ac}}\, h(\theta_{jz}) + K_{\mathrm{Ae}}]\, dz \end{aligned}\right\} \quad (1)$$

where K_{Ts}, K_{Rs}, and K_{As} (s = c, e) are empirically determined cutting and edge milling coefficients. $h(\theta_{jz})$ is the instantaneous chip thickness, given by

$$h(\theta_{jz}) = f_{\mathrm{t}}\ \sin\theta_{jz} \quad (2)$$

where f_{t} and θ_{jz} denote the feedrate and the element immersion angle, respectively, and θ_{jz} is defined as

$$\theta_{jz} = \theta + \sum_{j=0}^{N-1} \frac{2\pi}{N} - \frac{z\ \tan\beta}{R} \quad (3)$$

where N and R are the tooth number and the radius of the cutter, respectively. β and θ represent the helix and cutter rotation angles, respectively.

Milling Coefficient Calibration

For calibrating milling force coefficients here, a methodology is presented considering the influences of cutter geometry and cutting parameters on force distribution. The methodology is applied experimentally dividing the end mill into v number of discs. The average forces, $\overline{F}_X$ and $\overline{F}_Y$, are measured from specially devised milling tests for each disc element, and expressed as

$$\overline{F}_{\mathrm{q}} \equiv \overline{F}_{\mathrm{qc}}\, f_{\mathrm{t}} + \overline{F}_{\mathrm{qe}} \quad (4)$$

where $\overline{F}_{\mathrm{qc}}$ and $\overline{F}_{\mathrm{qe}}$ are the cutting and edge forces exerted on the disc at the slice, respectively. A second-order polynomial is used to describe a set of v pairs of cutting and edge forces $\{(z_1, \overline{F}_{\mathrm{qs},1}), (z_2, \overline{F}_{\mathrm{qs},2}), \ldots, (z_i, \overline{F}_{\mathrm{qs},i}), i \in [1, 2, \ldots, v]\}$ ($q = X,\ Y$ and s = c, e), as follows:

$$f_{\mathrm{qs}}(z) = c_{\mathrm{qs},0} + c_{\mathrm{qs},1}\ z_i + c_{\mathrm{qs},2}\ z_i^2 \quad (5)$$

where z_i is the axial coordinate of the ith disc. $c_{\mathrm{qs},0}$, $c_{\mathrm{qs},1}$, and $c_{\mathrm{qs},2}$ are the polynomial coefficients.

The force distribution is represented by free-body diagram of a disc element with height dz, as shown in Fig. 3. Since it has a small height, the distributed force is taken as a uniformly distributed force $\overline{F}_{\mathrm{qs}}(z)$ over the height dz, and then replaced by a load of magnitude $\overline{F}_{\mathrm{qs}}(z)\mathrm{d}z$. The cutting and edge shear forces at the location z and $z + \mathrm{d}z$ are denoted by $V_{\mathrm{qs}}(z)$ and $V_{\mathrm{qs}}(z) + \Delta V_{\mathrm{qs}}(z)$, respectively. The equilibrium equation of the forces acting on the element is written as

$$V_{\mathrm{qs}}(z) + \frac{\Delta V_{\mathrm{qs}}(z)}{\mathrm{d}z}\mathrm{d}z = V_{\mathrm{qs}}(z) - \overline{F}_{\mathrm{qs}}(z)\ \mathrm{d}z \quad (6)$$

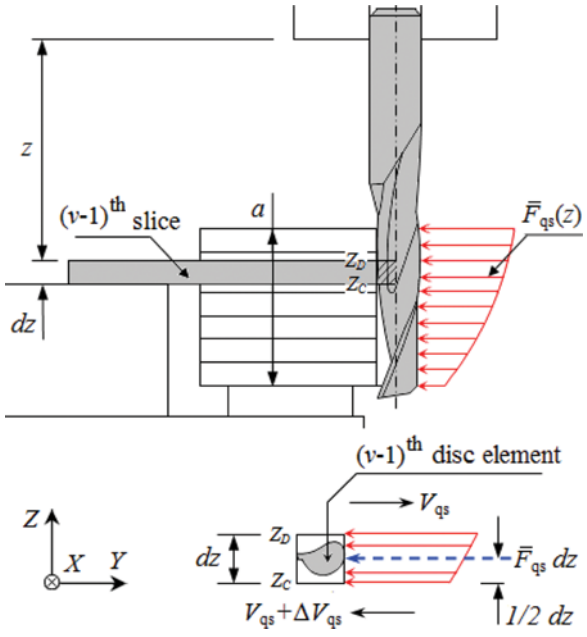

FIGURE 3.—End mill with chip load and free-body diagram of a disc element.

Integrating the cutting and edge shear forces on the height dz can be expressed as

$$V_{qs,z_D} - V_{qs,z_C} = -\int_{z_C}^{z_D} \bar{F}_{qs} dz \tag{7}$$

Thus, the cutting and edge shear forces (V_{qs}) are found by integrating the distributed force for axial cut depth (a):

$$V_{qs} = -\int_0^a f_{qs}(z) dz \tag{8}$$

The tangential ($F_{jz,T}$) and radial ($F_{jz,R}$) forces are resolved into x- and y-directions as follows:

$$\begin{Bmatrix} F_{jz,X}(\theta) \\ F_{jz,Y}(\theta) \end{Bmatrix} = \begin{bmatrix} -\cos\theta_{jz} & -\sin\theta_{jz} \\ \sin\theta_{jz} & -\cos\theta_{jz} \end{bmatrix} \begin{Bmatrix} F_{jz,T}(\theta) \\ F_{jz,R}(\theta) \end{Bmatrix} \tag{9}$$

The forces $F_{jz,X}$ and $F_{jz,Y}$ exerted by flute j at rotation angle θ are written as

$$\left.\begin{aligned} F_{jz,X}(\theta) &= \int_{z_{j,k-1}}^{z_{j,k}} \left\{ \frac{f_t}{2} \left[-K_{Tc} \sin 2\theta_{jz} - K_{Rc}(1-\cos 2\theta_{jz}) \right] \right. \\ &\quad \left. + \left[-K_{Te} \cos\theta_{jz} - K_{Re} \sin\theta_{jz} \right] \right\} dz \\ F_{jz,Y}(\theta) &= \int_{z_{j,k-1}}^{z_{j,k}} \left\{ \frac{f_t}{2} \left[K_{Tc}(1-\cos 2\theta_{jz}) - K_{Rc} \sin 2\theta_{jz} \right] \right. \\ &\quad \left. + \left[K_{Te} \sin\theta_{jz} - K_{Re} \cos\theta_{jz} \right] \right\} dz \end{aligned}\right\} \tag{10}$$

where $z_{j,k}$ and $z_{j,k-1}$ are the lower and upper integration boundaries, respectively. The sum of instantaneous forces at rotation angle θ is determined from the contributions of the forces exerted by all flutes as follows:

$$F_{sum,X}(\theta) = \sum_{j=0}^{N-1} F_{jz,X}(\theta); \quad F_{sum,Y}(\theta) = \sum_{j=0}^{N-1} F_{jz,Y}(\theta) \tag{11}$$

Combining Eqs. (4), (8), and (9), the cutting and edge coefficients are expressed as follows:

$$\begin{aligned} &K_{Tc}^{up} = \tfrac{8\pi}{Na}\left(\tfrac{-2V_{Xc}+\pi V_{Yc}}{\pi^2+4}\right); K_{Tc}^{down} = \tfrac{8\pi}{Na}\left(\tfrac{2V_{Xc}+\pi V_{Yc}}{\pi^2+4}\right); \\ &K_{Rc}^{up} = -2\left(\tfrac{K_{Tc}^{up}}{\pi} + \tfrac{4V_{Xc}}{Na}\right); K_{Rc}^{down} = 2\left(\tfrac{K_{Tc}^{down}}{\pi} - \tfrac{4V_{Xc}}{Na}\right); \\ &K_{Te}^{up} = \pi\left(\tfrac{-V_{Xe}+V_{Ye}}{Na}\right); K_{Te}^{down} = \pi\left(\tfrac{V_{Xe}+V_{Ye}}{Na}\right); \\ &K_{Re}^{up} = -K_{Te}^{up} - \tfrac{2\pi V_{Xe}}{Na}; K_{Re}^{down} = K_{Te}^{down} - \tfrac{2\pi V_{Xe}}{Na} \end{aligned} \tag{12}$$

where K_{ps}^{up}, and K_{ps}^{down} (p = T, R and s = c, e) are the established coefficients for up and down milling, respectively.

RESULTS AND DISCUSSION

Milling Force Coefficients

The variations of force distributions dependent on cutting parameters and cutter geometry are important in improving machining accuracy since the forces vary along the flute in end milling. Figure 4 shows the distributions of the cutting and edge components for $D = 12$ mm and $\gamma_n = 15°$ end mill. It is seen that the cutting and edge forces vary parabolically along the cutting part of the cutter, that is, the cutting and edge forces increase over the axial cut depth because of helical flutes. For the calibration of coefficients, these variations are defined through second-order polynomial equations. The cutting and edge shear forces are then calculated using Eq. (8).

Figure 5 shows the effects of cutting parameters and cutter geometry on milling coefficients. Milling type is investigated as the most important parameter. It is seen that the calibrated coefficients depend on cutting conditions as well as cutter-workpiece pair. In other words, the milling tests result in different values of the coefficients, which are performed under different cutting conditions. Cutter geometry also has a significant influence on coefficients. The coefficients identified for three different rake angles decrease with increasing rake angle in all cases of down milling while no such trend is observed in up milling.

Milling Force Verification

The accuracy of milling forces predicted using the milling coefficients identified from the suggested methodology has been verified through the comparison of forces measured. The tests were performed on Al7075-T651 blocks without coolant, at constant cutting speed, at different feedrates, and at constant axial cut depth 1.5

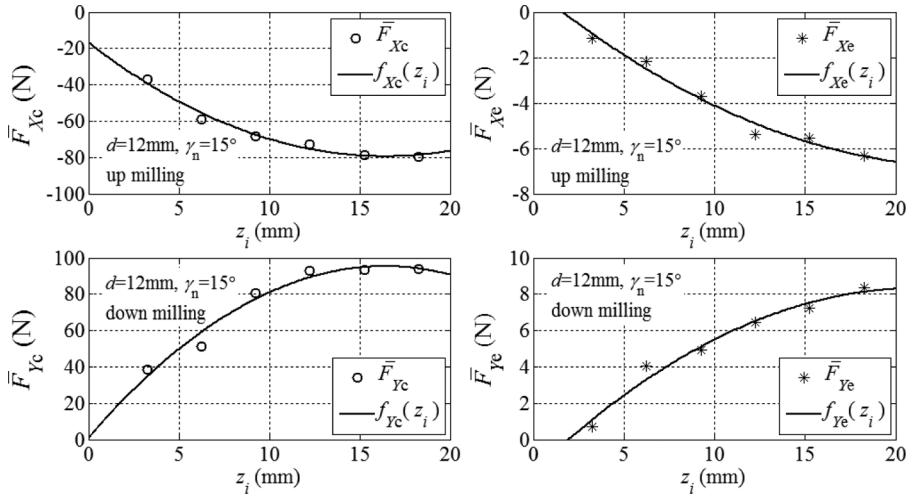

FIGURE 4.—Variations of cutting ($\bar{F}_{Xc}$, $\bar{F}_{Yc}$) and edge ($\bar{F}_{Xe}$, $\bar{F}_{Ye}$) forces.

times greater than the cutter diameter. The cutters were two-fluted carbide end mills with different rake angles and diameters. Table 1 shows the performance of average cutting forces mechanistically identified from the suggested methodology. As seen in Table 1, the mean absolute deviations of the predicted forces F_X and F_Y are 6.9% and 5.1%, respectively. The highest percentage deviation is obtained lesser than 15% for the predicted forces, apart from Test 12. These results indicate that the suggested methodology provides excellent accuracy rates for the cutting force predictions.

Figures 6 and 7 show instantaneous measured and predicted milling forces in 1.5 cutter revolutions for half-immersion up and down milling, respectively. It is observed that the milling forces that are predicted depending upon the coefficients identified mechanistically by the designed mechanism agree well with the measured forces. The slight deviations between measured and predicted forces can be associated with deflections and cutter runout. Furthermore, Fig. 5 indicates that when each tooth begins to cut in up milling, F_Y comes up to about 900 N and decreases to about 100 N at the end of the process. This circumstance will be imprinted on the surface as dimensional error. As seen in Fig. 6, a similar case is observed in down milling.

The average force approach in Ref. [21] is also considered to demonstrate the validity of the suggested methodology. The effect of the cutting-force distribution is neglected to establish the milling coefficients using the approach in Ref. [21] based on the average forces determined from the slot milling data. However, in the suggested methodology, the effect of force distribution is considered to determine the milling coefficients through a presently developed mechanism. Thus, the milling coefficients given in Fig. 4 are calibrated substituting the cutting (V_{Xc}, V_{Yc}) and edge (V_{Xe}, V_{Ye}) shear forces into Eq. (12), which are determined from the suggested methodology. The patterns of milling forces simulated by the

TABLE 1.—Comparison of measured and predicted cutting forces.

						F_X (N)			F_Y (N)		
Test no.	V (m/min)	f_t (mm/tooth)	Milling type	D mm	γ_n (°)	Measured	Predicted	Deviation (%)	Measured	Predicted	Deviation (%)
1	30	0.04	Up	12	15	−130.6	−139	6.4	277	276.5	0.2
2		0.08			15	−269.8	−277.9	3	524.4	553	5.5
3		0.12			10	−570	−598.3	5	948.5	937.4	1.2
4	30	0.04	Down	12	5	−266.1	−244.1	8.3	340.7	336.2	1.3
5		0.08			10	−395.9	−434.9	9.9	536.3	578.9	7.9
6		0.12			5	−802	−732.2	8.7	1004	1008.7	0.5
7	30	0.04	Up	10	10	−145.5	−144	1	249.2	261	4.7
8		0.08			10	−277.7	−288	3.7	465	522	12.3
9		0.12			5	−424.1	−419.4	1.1	642.5	685.8	6.7
10	30	0.04	Down	8	10	−103.7	−88.3	14.9	223.4	231.4	3.6
11		0.08			15	−158.3	−149.8	5.4	373	411.8	10.4
12		0.12			10	−311.6	−265	15	648.1	694.1	7.1
			Mean absolute deviation					6.9			5.1

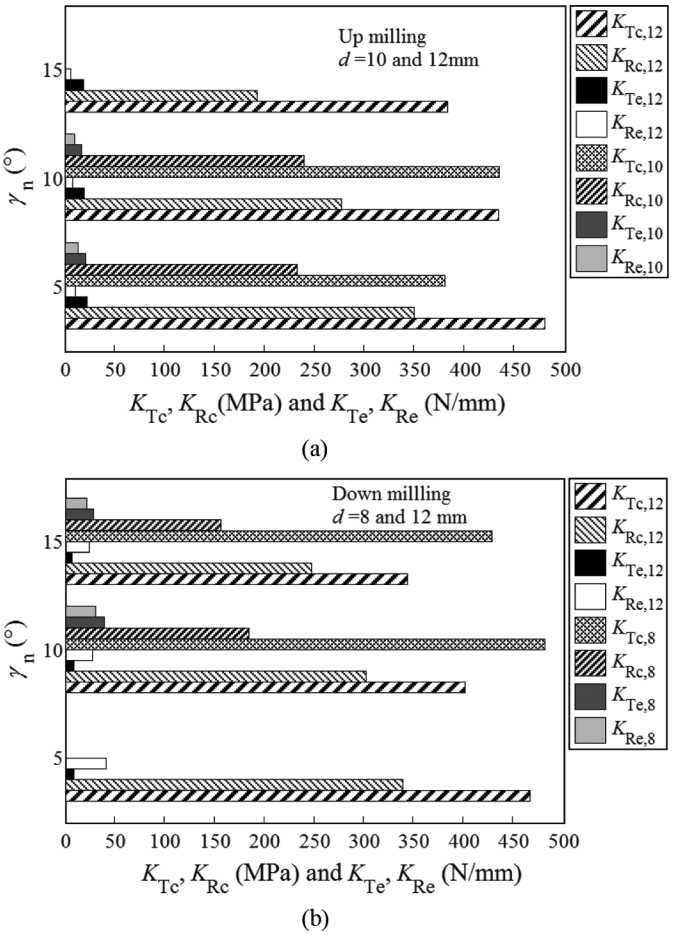

FIGURE 5.—Calibrated cutting and edge coefficients.

suggested methodology exhibit a better fit with the experimental forces than those obtained from the approach in Ref. [21]. Consequently, the milling forces predicted through the force distribution methodology are more accurate than those based on the average force approach.

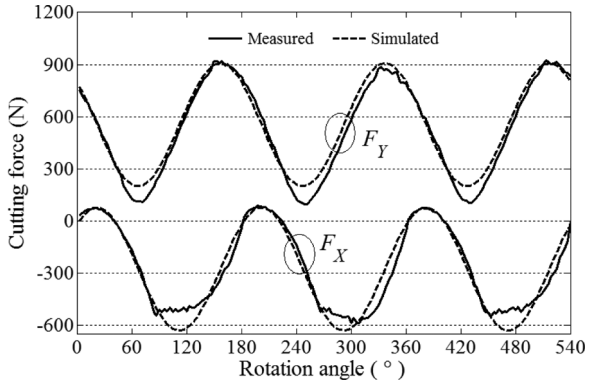

FIGURE 6.—Measured and simulated forces for up milling (Test 2).

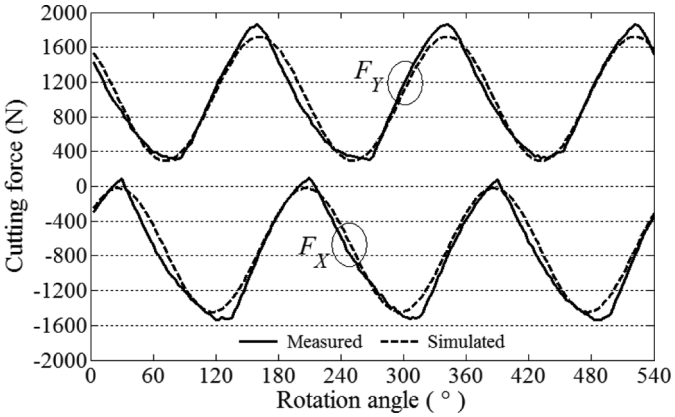

FIGURE 7.—Measured and simulated forces for down milling (Test 6).

CONCLUSIONS

This study improves the prediction of milling forces by suggesting a novel methodology to evaluate the milling coefficients in side milling. The advantage of the methodology is that the milling coefficients are established from the mechanistic model extended by experimentally identifying the force distribution along the cutting part of the cutter according to the influences of cutter geometry and cutting parameters. This contributes to improving the dimensional accuracy of sidewall surfaces, especially dies/molds, through cutting force knowledge. Relations between load and shear together with mechanics of end milling are examined to establish the milling coefficients, which are functions of the cutting and edge force components exerted by a disc element. Based on the newly developed experimental mechanism, the suggested methodology is validated by conducting verification tests. It is found that the results of the force distribution methodology are substantially in agreement with the findings achieved through verification tests. Consequently, it is necessary to be determined from the force distribution of the milling coefficients in milling processes where the chip thickness varies along the cutter axis.

REFERENCES

1. Hao, Z.P.; Lu, Y.; Gao, D.; Fan, Y.H.; Chang, Y.L. Cutting parameter optimization based on optimal cutting temperature in machining Inconel718. *Materials and Manufacturing Process* **2012**, *27* (10), 1084–1089.
2. Quintana, G.; De Ciurana, J.; Ribatallada, J. Surface roughness generation and material removal rate in ball end milling operations. *Materials and Manufacturing Process* **2010**, *25* (6), 386–398.
3. Li, H.Z.; Zhang, W.B.; Li, X.P. Modelling of cutting forces in helical end milling using a predictive machining theory. *International Journal of Mechanical Sciences* **2001**, *43*, 1711–1730.
4. Fontaine, M.; Moufki, A.; Devillez, A.; Dudzinski, D. Modelling of cutting forces in ball-end milling with tool–surface inclination. Part I: predictive force model and experimental validation. *Journal of Materials Processing Technology* **2007**, *189*, 73–84.

5. Sun, Y.; Ren, F.; Guo, D.; Jia, Z. Estimation and experimental validation of cutting forces in ball-end milling of sculptured surfaces. *International Journal of Machine Tools and Manufacture* **2009**, *49*, 1238–1244.
6. Hosseini, A.; Imani, B.M.; Kishawy, H.A. Mechanistic modelling for cutting with serrated end mills–a parametric representation approach. *Proceedings of the Institution of Mechanical Engineers, Part B: Journal of Engineering Manufacture* **2011**, *225*, 1019–1032.
7. Wan, M.; Pan, W.J.; Zhang, W.H.; Ma, Y.C.; Yang, Y. A unified instantaneous cutting force model for flat end mills with variable geometries. *Journal of Materials Processing Technology* **2014**, *214*, 641–650.
8. Dotcheva, M.; Millward, H.; Lewis, A. The evaluation of cutting-force coefficients using surface error measurements. *Journal of Materials Processing Technology* **2008**, *196*, 42–51.
9. Wan, M.; Zhang, W.H.; Tan, G.; Qin, G.H. New algorithm for calibration of instantaneous cutting-force coefficients and radial run-out parameters in flat end milling. *Proceedings of the Institution of Mechanical Engineers, Part B: Journal of Engineering Manufacture* **2007**, *221*, 1007–1019.
10. Wan, M.; Zhang, W.H.; Dang, J.W.; Yang, Y. A novel cutting force modelling method for cylindrical end mill. *Applied Mathematical Modelling* **2010**, *34*, 823–836.
11. Budak, E.; Altıntaş, Y.; Armerago, E.J.A. Prediction of milling force coefficients from orthogonal cutting data. *Transactions of the ASME Journal of Manufacturing Science and Engineering* **1996**, *118*, 216–224.
12. Gonzalo, O.; Jauregi, H.; Uriarte, L.G.; López De Lacalle, L.N. Prediction of specific force coefficients from a FEM cutting model. *International Journal of Advanced Manufacturing Technology* **2009**, *43*, 348–356.
13. Gonzalo, O.; Beristain, J.; Jauregi, H.; Sanz, C. A method for the identification of the specific force coefficients for mechanistic milling simulation. *International Journal of Machine Tools and Manufacture* **2010**, *50*, 765–774.
14. Wang, B.S.; Zuo, J.M.; Wang, M.L.; Hou, J.M. Prediction of milling force based on numerical simulation of oblique cutting. *Materials and Manufacturing Processes* **2012**, *27*, 1011–1016.
15. Cardoso, P.; Davim, J.P. Optimization of surface roughness in micromilling. *Materials and Manufacturing Process* **2010**, *25* (10), 1115–1119.
16. Srinivasa, Y.V.; Shunmugam, M.S. Mechanistic model for prediction of cutting forces in micro end-milling and experimental comparison. *International Journal of Machine Tools and Manufacture* **2013**, *67*, 18–27.
17. Rao, S.; Shunmugam, M.S. Analytical modeling of micro end-milling forces with edge radius and material strengthening effects. *Machining Science and Technology: An International Journal* **2012**, *16* (2), 205–227.
18. Afazov, S.M.; Ratchev, S.M.; Segal, J. Prediction and experimental validation of micro-milling cutting forces of AISI H13 steel at hardness between 35 and 60 HRC. *International Journal of Advanced Manufacturing Technology* **2012**, *62*, 887–899.
19. Özel, T.; Liu, X. Investigations on mechanics-based process planning of micro-end milling in machining mold cavities. *Materials and Manufacturing Processes* **2009**, *24* (12), 1274–1281.
20. Kline, W.A.; DeVor, R.E.; Shareef, I.A. The prediction of surface accuracy in end milling. *Transactions of the ASME Journal of Engineering for Industry* **1982**, *104*, 272–278.
21. Altintas, Y.; Spence, A. End milling force algorithms for CAD systems. *Annals of the CIRP* **1991**, *40*, 31–34.